


## RESEARCH ARTICLE OPEN ACCESS

# Unravelling Plasma Extracellular Vesicle Diversity With Optimised Spectral Flow Cytometry

Daniela Boselli<sup>1</sup> | Francesca Clemente<sup>1</sup> | Simona Di Terlizzi<sup>1</sup> | Christina Pagiatakis<sup>2,3</sup> | Laura Papa<sup>2</sup> | Genny Del Zotto<sup>4</sup> | Chiara Villa<sup>1,5</sup> | Giuseppe Alvise Ramirez<sup>6,7</sup> | Norma Maugeri<sup>5,7</sup> | Angelo A. Manfredi<sup>5,6,7</sup> | Achille Anselmo<sup>1,5</sup> 

<sup>1</sup>Experimental Imaging Center, FRACTAL, Flow cytometry Resource, Advanced Cytometry Technical Applications Laboratory, IRCCS Ospedale San Raffaele, Milan, Italy | <sup>2</sup>Department of Cardiovascular Medicine, IRCCS Humanitas Research Hospital, Rozzano, Milan, Italy | <sup>3</sup>Department of Biotechnology and Life Sciences, University of Insubria, Varese, Italy | <sup>4</sup>Department of Research and Diagnostics, IRCCS Istituto Giannina Gaslini, Genoa, Italy | <sup>5</sup>Università Vita-Salute San Raffaele, Milan, Italy | <sup>6</sup>Unit of Immunology, Rheumatology, Allergy and Rare Diseases, IRCCS Ospedale San Raffaele, Milan, Italy | <sup>7</sup>Division of Immunology, Transplantation and Infectious Diseases, IRCCS Ospedale San Raffaele, Milan, Italy

**Correspondence:** Achille Anselmo ([anselmo.achille@hsr.it](mailto:anselmo.achille@hsr.it))

**Received:** 27 September 2024 | **Revised:** 27 February 2025 | **Accepted:** 13 March 2025

**Funding:** This work was supported by the European Union - Next Generation EU - NRRP M6C2 - Investment 2.1 Enhancement and strengthening of biomedical research in the NHS. Project N° PNRR-MR1-2022-12376638, PI Prof. Angelo Manfredi.

**Keywords:** antibody | extracellular vesicle | fluorochrome | immunophenotyping | plasma | SLE | spectral flow cytometry | unsupervised analysis

## ABSTRACT

Extracellular vesicles (EVs) are crucial for intercellular communication and are found in various biological fluids. The identification and immunophenotyping of such small particles continue to pose significant challenges. Here, we have developed a workflow for the optimisation of a next-generation panel for in-depth immunophenotyping of circulating plasma EVs using spectral flow cytometry. Our data collection followed a multistep optimisation phase for both instrument setup and 21-colour panel design, thus maximising fluorescent signal recovery. This spectral approach enabled the identification of novel EV subpopulations. Indeed, besides common EVs released by erythrocytes, platelets, leukocytes and endothelial cells, we observed rare and poorly known EV subsets carrying antigens related to cell activation or exhaustion. Notably, the unsupervised data analysis of major EV subsets revealed subpopulations expressing up to five surface antigens simultaneously. However, the majority of EVs expressed only a single surface antigen, suggesting they may not fully represent the phenotype of their parent cells. This is likely due to the small surface area or the biogenesis of EVs rather than antibody steric hindrance. Finally, we tested our workflow by analysing the plasma EV landscape in a cohort of systemic lupus erythematosus (SLE) patients. Interestingly, we observed a significant increase in CD54<sup>+</sup> EVs, supporting the notion of elevated circulating ICAM under SLE conditions. To our knowledge, these are the first data highlighting the importance of a spectral flow cytometry approach in deciphering the heterogeneity of plasma EVs paving the way for the routine use of a high-dimensional immunophenotyping in EV research.

Achille Anselmo is the lead contact.

This is an open access article under the terms of the [Creative Commons Attribution-NonCommercial-NoDeriv](https://creativecommons.org/licenses/by-nc-nd/4.0/) License, which permits use and distribution in any medium, provided the original work is properly cited, the use is non-commercial and no modifications or adaptations are made.

© 2025 The Author(s). *Journal of Extracellular Biology* published by Wiley Periodicals LLC on behalf of International Society for Extracellular Vesicles.

## 1 | Introduction

EVs are naturally occurring nanocarriers released by virtually all cell types. They are crucial for intercellular communication and play non-redundant roles in the homeostasis of multicellular organisms. According to the recommendation of the International Society for Extracellular Vesicles (ISEV), EVs can be classified based on their physical features, such as density, size or origin (platelet EVs) (Théry et al. 2018, Welsh et al. 2023, Welsh et al. 2024). Upon fusion with the plasma membrane, EVs expose antigens originating from their parental cells, together with negatively charged phospholipids and membrane-associated glycoproteins (Théry et al. 2018, Welsh et al. 2023, Yáñez-Mó et al. 2015, Dasgupta et al. 2009). Once released, EVs interact with the surrounding environment and represent a source of biomolecules, including lipids, metabolites, nucleic acids (ncRNAs) along with cytokines, chemokines and growth factors (Yáñez-Mó et al. 2015, Anselmo et al. 2021, Hunter et al. 2008, Diehl et al. 2012, Verderio et al. 2018, Haraszti et al. 2016). Moreover, increasing evidence suggests the presence of a protein corona around the EV surface upon exposure to body fluids (Tóth et al. 2021, Heidarzadeh et al. 2023). Although several proteins, including Annexins, Lamp1 or tetraspanins have been proposed as potential markers of EVs, their universality remains unclear and is not yet widely accepted (Théry et al. 2018, Welsh et al. 2024).

EV shedding increases inflammation, hypoxia and mechanical stress (Anselmo et al. 2021, Vion et al. 2013). Moreover, EVs accumulate in various body fluids including blood and urines where they serve as indicators of the immediate metabolic state and biological traits of the cells from which they originate (Théry et al. 2018, Welsh et al. 2023, Welsh et al. 2024, Yáñez-Mó et al. 2015, Xu et al. 2016).

As a result, EVs have emerged as valuable biomarkers in complex human diseases, including metabolic syndromes, cancer, cardiovascular disorders and autoimmune conditions (Loyer et al. 2014, Withrow et al. 2016, Robbins et al. 2016, Zhao et al. 2020, Kok and Yu 2020). However, accurately identifying, characterising and quantifying these small particles still remains a challenge for researchers in this field.

Flow cytometry is one of the most widespread techniques used for EV analysis (Cossarizza et al. 2019, Arraud et al. 2016, Welsh et al. 2021). However, the small size of EVs and the low abundance of certain surface antigens present challenges for conventional flow cytometry approaches. This has made necessary tailored instrument set-up (Cook et al. 2023) as well as the development of specialised instrumentation for EV analysis, vesicle-specific technologies and experimental design (Gul et al. 2022).

The newborn spectral flow cytometry addresses some of the drawbacks of conventional flow cytometry by measuring the complete emission spectrum and subsequently deconvoluting it to identify individual fluorochrome signals (Robinson 2019, Nolan 2022, Novo 2022). The application of spectral flow cytometry for multicolour EV analysis reduces spreading error and minimises spectral overlap among fluorochromes, thus improving the detection of weak fluorescent signals (Panagopoulou et al. 2020). Moreover, spectral analysers equipped with high quantum efficiency and low electronic noise detectors, such as avalanche

photodiodes, along with Violet Side Scatter (VSSC), enhance sensitivity for detecting small particles (Gul et al. 2022, McVey et al. 2018, Brittain et al. 2019).

Systemic lupus erythematosus (SLE) is a prototypic systemic autoimmune disease, characterised by clinical heterogeneity and widespread multi-organ involvement (Tsokos 2011, Rahman and Isenberg 2008). Recent evidence proposes EVs as active players in the pathogenesis and clinical complications of SLE (Nielsen et al. 2016), as well as potential biomarkers for disease activity (Mobarrez et al. 2019, Perez-Hernandez and Cortes 2015, Viñuela-Berni et al. 2015, López et al. 2017, Burbano et al. 2019, Crawford et al. 2023, Karlsson et al. 2023, Anees et al. 2024). Moreover, EVs serve as a reservoir of extracellular DNA, which is the primary autoantigen in SLE. This DNA can originate from apoptotic bodies derived from dying cells or be actively released as EVs by activated cells, in which mitochondria might represent the main constituents. These EV-associated components circulate systemically via biological fluids, contributing to the specific organ features observed in SLE patients (Pisetsky 2024).

In this manuscript, we performed a comprehensive immunophenotyping panel to identify plasma EVs through multicolour spectral flow cytometry. This followed an instrument optimisation phase and fluorochrome performance tracking tailored for EV analysis, both aimed at enhancing EV detection. The unsupervised analysis, focusing on the most abundant EV subsets, revealed a high degree of circulating EV heterogeneity, including rare and previously poorly characterised subpopulations.

Moreover, the immunophenotype of the EVs indicates that they do not entirely reflect the characteristics of their parent cells. This difference seems to arise from factors like the limited surface area of EVs or their distinct biogenesis, rather than being due to antibody steric hindrance. Finally, we validated this approach by studying plasma EVs in a pilot cohort of SLE patients as compared to healthy donors (HDs), establishing a reliable and useful tool for identifying new circulating biomarkers associated with systemic autoimmunity.

## 2 | Materials and Methods

### 2.1 | Study Population: SLE Patients and HDs

Upon written informed consent, eight patients with SLE according to the 2012 SLE International Collaborating Clinics (SLICC) criteria (Petri et al. 2012) and eight sex- and age-matched HDs were enrolled in the Autoimmuno-mol protocol. The protocol conforms to the Declaration of Helsinki and has been approved by the San Raffaele Hospital Institutional Review Board with reference number 02/2013/INT. Collected clinical data from patients with SLE encompassed disease duration and SLE clinical manifestations over the entire disease course. The serological profile of patients with SLE was also characterised by determining the frequency of anti-DNA, anti-cardiolipin, anti-beta-2-glycoprotein I, anti-extractable nuclear antigens antibodies along with the presence of lupus anticoagulant and of low complement levels in patient history. Data regarding positive anti-DNA antibodies and complement levels were also collected at the time of enrolment. Disease activity and accrued damage were estimated through the SLE disease activity index 2000 (SLEDAI-2K) and the

SLICC/American College of Rheumatology damage index (SDI) (Stoll et al. 1996, Gladman et al. 2002), respectively. Patients were classified as being or not in remission according to the DORIS definitions (van Vollenhoven et al. 2021).

## 2.2 | Primary Cell Isolation

Venous blood was collected, after informed consent was obtained, from healthy volunteers, who denied having received any medication for at least 2 weeks. Venous blood was obtained using a 19-gauge butterfly needle and collected in EDTA-containing Vacutainers. Samples were immediately processed as previously described to purify neutrophils and PBMCs (Manfredi et al. 2022, Maugeri et al. 2014, Maugeri et al. 2006). Briefly, samples were centrifuged at  $180 \times g$  for 15 min at  $18^{\circ}\text{C}$  and platelet-rich plasma was removed. Neutrophils and PBMCs were isolated from the remaining blood by Dextran sedimentation followed by Ficoll-Hypaque gradient. PBMCs were retrieved from the interphase of Ficoll-Hypaque whilst neutrophils were retrieved from the bottom layer. Contaminating erythrocytes were removed by hypotonic lysis. Cells were washed and resuspended in HEPES-Tyrode buffer (pH 7.4), containing 1 mM  $\text{CaCl}_2$  and the concentration was adjusted at 5000 cells/ $\mu\text{L}$ . All procedures for leukocyte isolation were performed at  $4^{\circ}\text{C}$ .

## 2.3 | Isolation of EVs From In Vitro Stimulated Neutrophils and PBMCs

PBMCs were stimulated using 1  $\mu\text{g}/\text{mL}$  PHA for 72 h at  $37^{\circ}\text{C}$ . Neutrophils were stimulated with IL-8 (100 ng/mL) or with fMLP (1  $\mu\text{M}$ ) or vehicle (Hepes Tyrode) for 1 h at  $37^{\circ}\text{C}$ .

After stimulation, samples were centrifuged at  $13,000 \times g$  for 15 min at  $4^{\circ}\text{C}$  and the supernatant was frozen at  $-80^{\circ}\text{C}$  until analysis.

EV isolation from both supernatants was performed by centrifuging them at  $15,000 \times g$  for 45 min at  $4^{\circ}\text{C}$ . Then, the pellets enriched in EVs were re-suspended using 0.22  $\mu\text{m}$  pre-filtered PBS without calcium and magnesium ( $\text{PBS}^{-/-}$ ).

## 2.4 | Platelet-Free Plasma Preparation and Storage

Venous blood was obtained using a 19-gauge butterfly needle and collected into an EDTA-containing Vacutainer. Samples were immediately centrifuged for 15 min,  $800 \times g$  at room temperature (RT). Plasma was removed and centrifuged again for 5 min at  $13,000 \times g$  and the supernatant was collected and frozen at  $-80^{\circ}\text{C}$  in single-use aliquots with suitable volumes for the planned downstream analyses to avoid multiple freeze-thaw cycles. If necessary, plasma sample transfer was performed using dry ice.

## 2.5 | Sample Staining and Acquisition Through Spectral Flow Cytometry

Sample staining was performed using saturating concentration of pre-titrated monoclonal antibodies (mAbs). mAbs were cen-

trifuged at  $15,000 \times g$  for 30 min at  $4^{\circ}\text{C}$  and 0.22  $\mu\text{m}$  filtered. Single staining reference controls were prepared using FSP CompBeads (Cytek) following manufacturer instructions. Cell membrane fragments were excluded from the analysis by using Phalloidin Alexa 647 (Invitrogen). Three kinds of samples were analysed: plasma EVs, PBMC-derived EVs and neutrophil-derived EVs.

For Plasma EVs: 25  $\mu\text{L}$  of the sample was first diluted 1:4 by adding 0.22  $\mu\text{m}$  pre-filtered  $\text{PBS}^{-/-}$ . Then the diluted plasma was stained using the list of mAbs reported in Table S1.

For PBMC-derived and neutrophil-derived EVs: 50  $\mu\text{L}$  of sample was first diluted 1:2 by adding 0.22  $\mu\text{m}$  pre-filtered  $\text{PBS}^{-/-}$ . Then the diluted sample was stained using the list of mAbs reported in Tables S1–S3 or S4.

All EV samples were stained for 1 h at RT in the dark. To minimise swarm effect all samples were further diluted using 0.22  $\mu\text{m}$  filtered  $\text{PBS}^{-/-}$ . All gated regions were restrictively drawn referring to fluorescence minus one (FMO) control or the appropriate isotype controls.

Data acquisition was performed using Aurora Cytek equipped with 5 lasers (355, 405, 488, 561 and 640 nm). Before any acquisition, an instrument quality check was done using SpectroFlo QC Beads (Cytek). Fluidic stability was checked daily to minimise fluctuations in the fluorescent signal recovery. Light scatter parameters were set up using hollow organo-silica Verity Shells beads (374 and 189 nm) (Exometry). To relate scatter signals to diameter of particles, Rosetta Calibration (version v1.23, Exometry) was used following manufacturer instructions. Unmixing was done using the SpectroFlo software. A conventional 2D manual gating strategy was performed using FloJo software (version 10.8.1).

## 2.6 | Unsupervised Data Analysis

Flow cytometry data were imported into FlowJo software (version 10.8.1) to adjust spectral overlap; Phalloidin positive events were excluded from the analysis. Random down-sampling of 700, 600 and 700 events was performed for  $\text{CD144}^{+}$  EVs,  $\text{CD61}^{+}$  EVs and  $\text{CD15}^{+}$  EVs respectively. The data were exported as Flow cytometry standard (FCS) files for further analysis using R software (version 4.3.1). Sample batches were read using `read.flowSet` from the R package `flowCore` (2.14.1). We applied the logicle transformation, which allows the use of multiple samples to estimate transformation parameters. To reduce batch effects due to technical rather than biological variation, we normalised the signal of each marker using the `gaussNorm` function of the `flowStat` package (4.14.1). After batch-specific pre-processing, samples were concatenated into a `SingleCellExperiment` object in R using the `prepData` function of the `CATALYST` R package. Dimensionality reduction by uniform manifold approximation and projection (UMAP) was subsequently applied to enable the visualisation of the relative proximities of EVs within reduced dimensions. We performed high-resolution, unsupervised clustering and meta-clustering using `FlowSOM` (2.10.0) and `ConsensusClusterPlus` (1.66.0) packages, following the workflow described by Nowicka et al. (2017). The  $\text{CD144}^{+}$ ,  $\text{CD61}^{+}$  and  $\text{CD15}^{+}$  EVs were clustered based on the expression of the following

activation/exhaustion markers: CD62P, CD25, CD95, PD-1, CD54, CD163, CD206, HLA-DR, PD-L1 and IgM.

## 2.7 | Statistical Analysis

Comparisons among SLE patients and healthy controls were evaluated by the Unpaired T test.

Statistical analyses were performed using GraphPad PRISM

## 3 | Results

### 3.1 | Optimisation of Settings for Enhanced EV Detection

Once a flow cytometry analyser is installed, the default values for fluorescence and scatter detection are optimised for cell detection, primarily leukocytes, during both the instrument qualification (IQ) and operational qualification (OQ) phases. Therefore, an additional optimisation phase is required for the detection of small particles. To this end, we first performed a 405 nm light scatter calibration using Verity Shell beads, organo-silica beads that have a refractive index distribution and light scattering properties more similar to EVs than traditional polystyrene beads. This calibration allowed us to optimise the light scatter parameters, thereby improving our ability to discriminate EV-like events from the electronic noise. More in detail, we observed a change in the absolute count of the 374 nm beads across light scatter settings. Notably, the optimal sensitivity for 405 nm light scatter was achieved with a gain set between 1500 and 2500 (Figure 1A), enabling the discrimination of 189 nm beads from electronic noise (Figure S1A). As expected, this setup also allowed for the detection of plastic beads smaller than 189 nm (Figure S1B).

As a second step, we optimised the fluorescence settings to maximise detection sensitivity under our experimental conditions. Specifically, we quantified the amount of CD4<sup>+</sup> derived EVs obtained from in vitro stimulated peripheral blood mononuclear cells (PBMCs). We confirmed the vesicular origin of the EVs released by stimulated PBMCs by performing western blot analysis for luminal and surface vesicular antigens (namely, CD9, CD81, flotillin, ALIX and TSG101) (Figure S2A). The overall size of these EV-like particles was defined through Nanoparticle Tracking Analysis (NTA), which revealed peaks at 164, 307 and 446, suggestive of a heterogeneous EV population (Figure S2B). These EVs were further stained using the same anti-human CD4 mAb conjugated with the fluorochromes listed in Table S1, across various fluorescent detector settings. (Figures 1B and S3).

Notably, the most sensitive setting did not correspond to the highest detector gain. Indeed, as showed in Figures 1B and S3, we selected an overall gain increase of 50% from the Instrument assay settings, defined by instrument QC, moreover, we applied the same gain increase across all the detectors to maintain the quality of the spectral unmixing and avoid misleading signal resolution. Additionally, to further phenotype CD4-derived EVs we investigated their CD63, CD9 and CD81 surface expression through spectral flow cytometry (Figure S4A). As expected, not all CD4-derived EVs displayed these tetraspanins on their surface,

supporting the notion of a lack of universal markers for EVs (Welsh et al. 2024). We used Rosetta Calibration technology to relate scatter signals of these EV subsets to their diameter (van der Pol et al. 2021). The data in Figure S4B are consistent with observations made using NTA, thereby revealing a heterogeneous size distribution of CD4-derived EVs with the majority ranging between 140 and 500 nm.

Finally, we optimised electronic acquisition settings such as area scaling factor (ASF) and window extension (WE) settings for EV analysis. For the identification of the best ASF setting (Figure 1C), which slightly differed from the default values, we used EVs obtained from in vitro stimulated neutrophils. These EVs were stained using the same anti-human CD15 mAb conjugated with the fluorochromes listed in Table S3. The CD15<sup>+</sup> EVs showed the same size distribution as CD4<sup>+</sup> EVs (not shown). For the WE optimisation, we quantified neutrophil-derived EVs stained using anti-human CD15-APC at different WE values. Interestingly, by decreasing the WE from 6  $\mu$ s to 1–2  $\mu$ s, sensitivity increased as evidenced by the higher number of detected CD15<sup>+</sup> EVs (Figure 1D).

Notably best sample dilution conditions were defined to avoid swarm effect within our experimental conditions (Figure S5).

Overall, whilst we cannot formally exclude the possibility that small EVs (< 140 nm) were overlooked—leading to a focus mainly on large EVs—the use of EVs instead of beads for fluorescence and scatter calibration offers a viable alternative. This approach minimises the detrimental effects caused by refractive index differences among beads and EVs, thereby optimising instrument performance.

### 3.2 | Deep Immunophenotyping of Plasma EV

Human plasma contains a wide repertoire of circulating tissue-derived EVs. To capture this diversity, we developed a method for the detection of plasma-EVs released by various cell types using spectral flow cytometry. To this end, we used pre-diluted plasma to minimise sample manipulation thus preserving EV integrity and quantity. Of note, we analysed the plasma EV phenotype and size thereby confirming the expression of luminal and surface vesicular antigens as well as revealing peaks at 136, 207 and 437 (Figure S6A,B). To perform a landscape analysis of plasma-derived EVs, we designed a 21-colour panel including antibodies recognising both lineage and markers related to cell activation/exhaustion, conjugated with fluorochromes characterised by high uniqueness, resulting in low complexity of the spectral unmixing matrix (Table S1 and Figure S7A). Furthermore, we conducted an unmixing spreading error analysis of our colour palette to verify its low impact on the overall signal resolution (Figure S7B).

To ensure the fluorochromes listed in Table S1 had sufficient brightness for phenotyping EV-related surface antigens, we compared the amount of CD4<sup>+</sup> derived EVs obtained from the supernatant of in vitro stimulated PBMCs. This was done using the same anti-human CD4 mAb conjugated with all the fluorochromes potentially included in the panel. As shown in Figure 2A, all fluorochromes demonstrated sufficient brightness



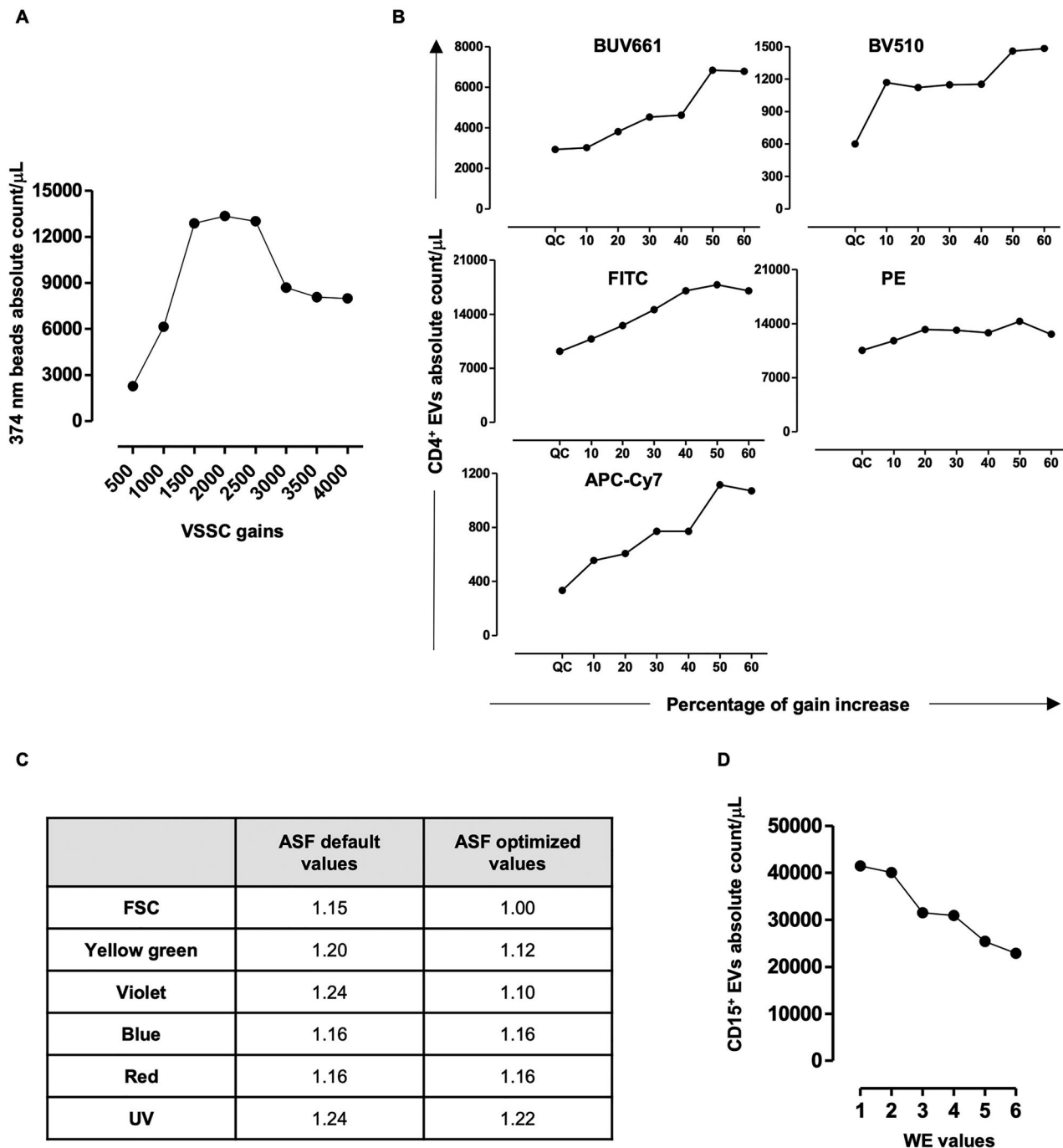


**FIGURE 1** | Optimisation of spectral flow cytometry settings for extracellular vesicle analysis. For 405 nm light scatter calibration setting: Hollow organo-silica Verity Shells beads were used for the set-up of the Aurora Cytex 405 nm light scatter (VSSC).  $5 \times 10^6$  of 374 nm beads were diluted in 500  $\mu$ L of PBS without calcium and magnesium (PBS<sup>-/-</sup>) and acquired at increasing 405 nm-light scatter detector setting (from 500 to 4000 gains). An absolute count of 374 nm beads at each 405 nm light scatter gain was reported (A). For fluorescence detector setting: EVs from in vitro stimulated PBMCs were stained using the same anti-human CD4 mAb conjugated with BUV661, BV510, FITC, PE and APC-Cy7 respectively. Samples were acquired using Cytex assay settings, defined by instrument QC and upon the following gain increase: 10%, 20%, 30%, 40%, 50% and 60%. The same gain increase was applied for all the detectors. Total number of CD4 positive events/ $\mu$ L were reported (B). For Area scaling factor optimisation: EVs from in vitro stimulated neutrophils were stained using the same anti-human CD15 antibody conjugated with BUV661, BV510, FITC, PE and APC respectively and analysed by varying instrument area scaling factor. Default and optimised ASF values were reported (C). For Window extension optimisation: EVs from in vitro stimulated neutrophils were stained using anti-human CD15 antibody conjugated with APC and analysed by varying instrument WE settings. EV absolute count at different WE values was reported (D). All data were representative of two independent observations.

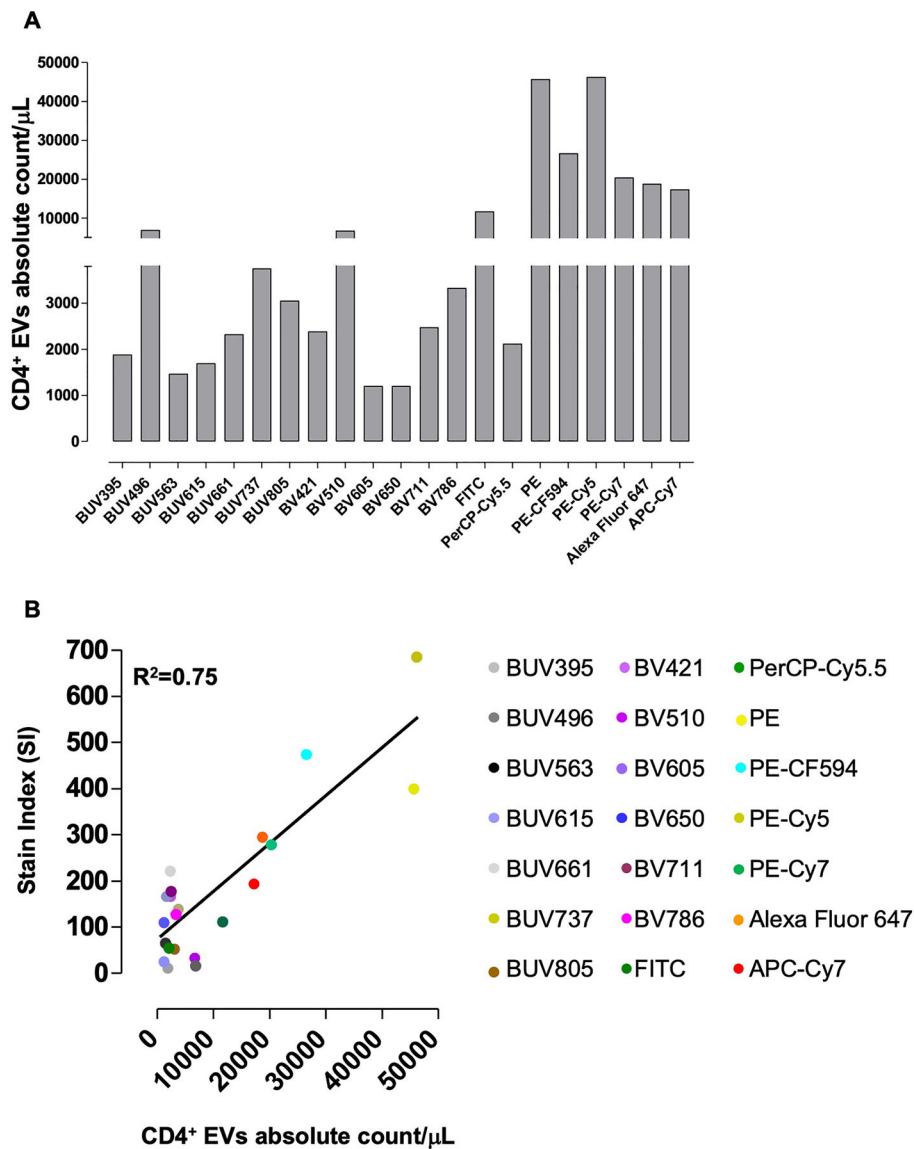


**FIGURE 2** | Correlation between EV absolute count and fluorochrome brightness. EVs from in vitro stimulated PBMCs were stained using the same anti-CD4 antibody conjugated with all the fluorochromes included in the panel. The total number of CD4<sup>+</sup> derived EVs and their correlation with fluorochrome brightness was reported in panels A and B, respectively.

to detect CD4<sup>+</sup> T cell-derived EVs, although some performed better than others. We then compared the EV count with the fluorochrome stain index, a parameter used to measure dye brightness, and observed a good direct correlation (Figure 2B). Based on this finding, we concluded that certain fluorochromes are more suitable for EV analysis than others. Thus, to maximise signal resolution, we assigned the dimmer fluorochromes to lineage markers and the brightest ones to activation/exhaustion markers.

With the feasibility of our panel design verified for plasma-EV analysis, we focused on the EV gating strategy. The identification of the main EV subsets was initially defined through a manual back-gating approach. We first excluded cell fragments (R2) from the analysis by using Phalloidin then we identified EVs expressing lineage markers such as platelet-derived EVs (CD61<sup>+</sup> events, R3), endothelium-derived EVs (CD144<sup>+</sup> events, R4), erythroid-derived EVs (CD235a<sup>+</sup> events; R6) and several subsets of leukocyte-

derived EVs (CD15<sup>+</sup>, CD56<sup>+</sup>, CD3<sup>+</sup>, CD14<sup>+</sup>, CD4<sup>+</sup>, CD20<sup>+</sup>, CD8<sup>+</sup> events; R7, R9, R10, R12, R13, R15, R16 respectively) (Figure 3). Of note, the antibodies recognising lineage antigens were highly specific, with an overall cross-reaction of < 10% (Table S4).

We further characterised EVs based on the surface expression of the following activation/exhaustion markers: PD-1 (R18), CD25 (R19), CD54 (R20), CD62P (R21), CD95 (R22), CD163 (R23), CD206 (R24), IgM (R25) PD-L1 (R26) and HLA-DR (R27) (Figure 3). As suggested by MIFlowCyt-EV framework guidelines (Welsh et al. 2021), we observed a reduction in the amount of well-expressed EV subsets upon either the sample serial dilution (Figure S8A) or Triton-X sample treatment (Figure S8B) thus supporting their vesicular origin.

The conventional 2D manual gating strategy described above could overlook and inadequately represent the entirety of the data. To address this topic, we adopted an unbiased approach

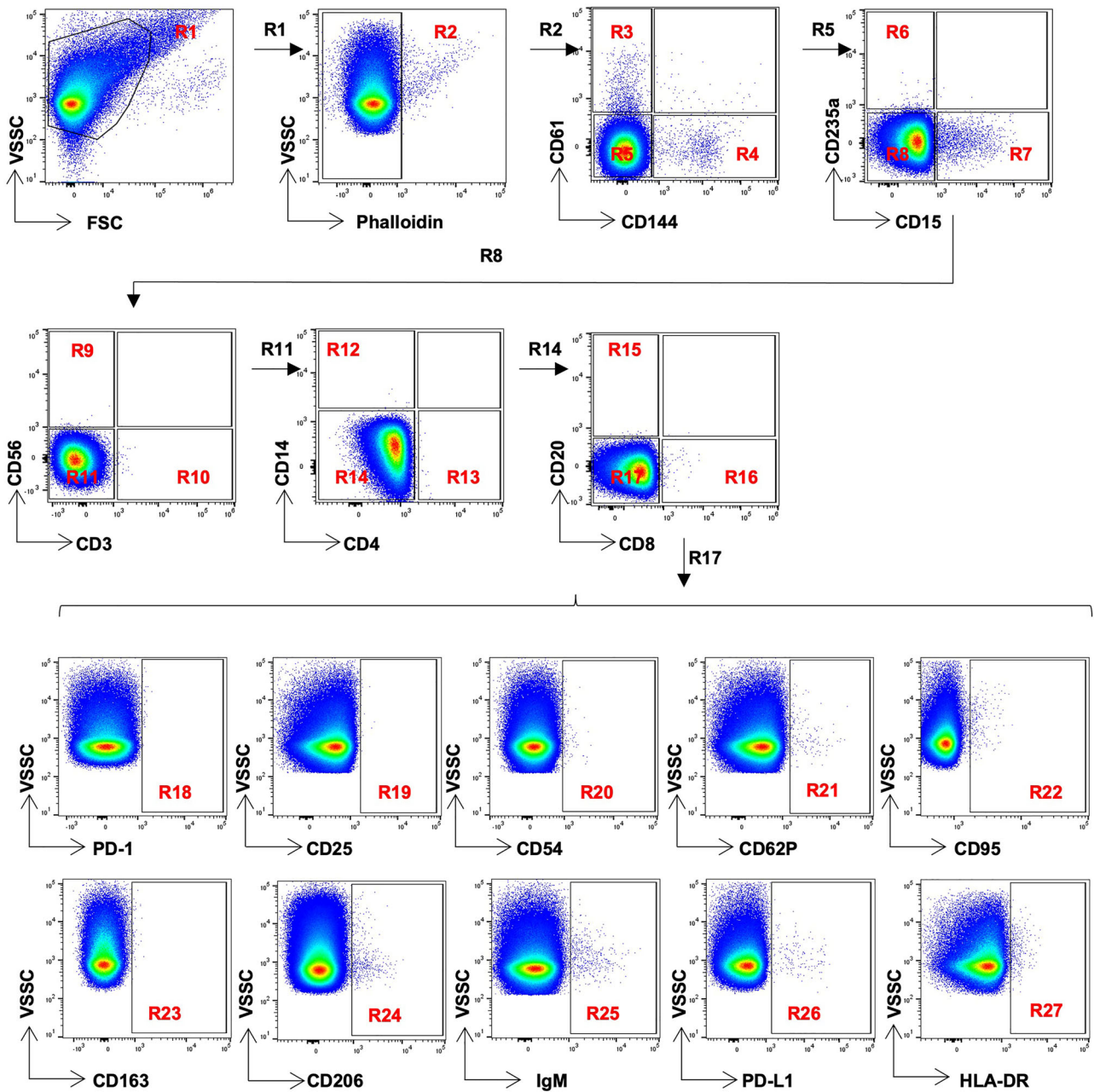


**FIGURE 3** | 2D manual gating strategy used to identify the main EV subsets from human plasma. EVs were gated based on FSC/405 nm VSSC properties (R1). Upon exclusion of cell fragments by using Phalloidin (R2), platelets and endothelial-derived EVs were identified as CD61<sup>+</sup> (R3) and CD144<sup>+</sup> EVs (R4). CD61<sup>+</sup>/CD144<sup>+</sup>/Phalloidin<sup>+</sup> events (R5), were analysed for the expression of CD235a and CD15 and erythrocyte-derived (R6) and neutrophils like (R7) EVs were identified. CD235<sup>+</sup>/CD15<sup>+</sup> (R8) events were assessed for CD56 and CD3 expression and NK-like (R9) and T cell-like (R10) derived EVs were recognised. On CD56<sup>+</sup>/CD3<sup>+</sup> gated events (R11), CD14 and CD4 were used to identify monocyte (R12) and CD4<sup>+</sup> (R13) derived EVs. On CD14<sup>+</sup>/CD4<sup>+</sup> gated events (R14), CD20 and CD8 were used to identify B cell-like (R15) and CD8<sup>+</sup> (R16) derived EVs. Finally, R17 gated events (CD20<sup>+</sup>/CD8<sup>+</sup>) were analysed for the expression of PD-1 (R18), CD25 (R19), CD54 (R20), CD62P (R21), CD95 (R22), CD163 (R23), CD206 (R24), IgM (R25), PD-L1 (R26) and HLA-DR (R27).

by using dimensionality reduction and FlowSOM clustering to explore the data comprehensively, focusing on the three primary EV subsets (CD144<sup>+</sup> EVs, CD61<sup>+</sup> EVs and CD15<sup>+</sup> EVs).

More interestingly, as shown in Figure 4, among the investigated EV subsets, we identified a predominant cluster expressing only the antigen selected for the unsupervised analysis, alongside several other clusters that exhibit the expression of more than

one antigen (33.6±7.6% among total CD144<sup>+</sup> EVs; 6.7±2.7% among total CD61<sup>+</sup> EVs; 7.9±2.4% among total CD15<sup>+</sup> EVs). Importantly, all identified clusters were validated through a manual gating strategy (Figure S9A-C). CD144<sup>+</sup>, CD61<sup>+</sup> and CD15<sup>+</sup> EVs showed no relevant differences either in size range, as defined using the Rosetta calibration kit (CD144<sup>+</sup> EVs: 140–400 nm; CD61<sup>+</sup> EVs: 140–450 nm; CD15<sup>+</sup> EVs: 140–400 nm), or in the surface expression of CD9, CD63 and CD81, except for the % of CD9

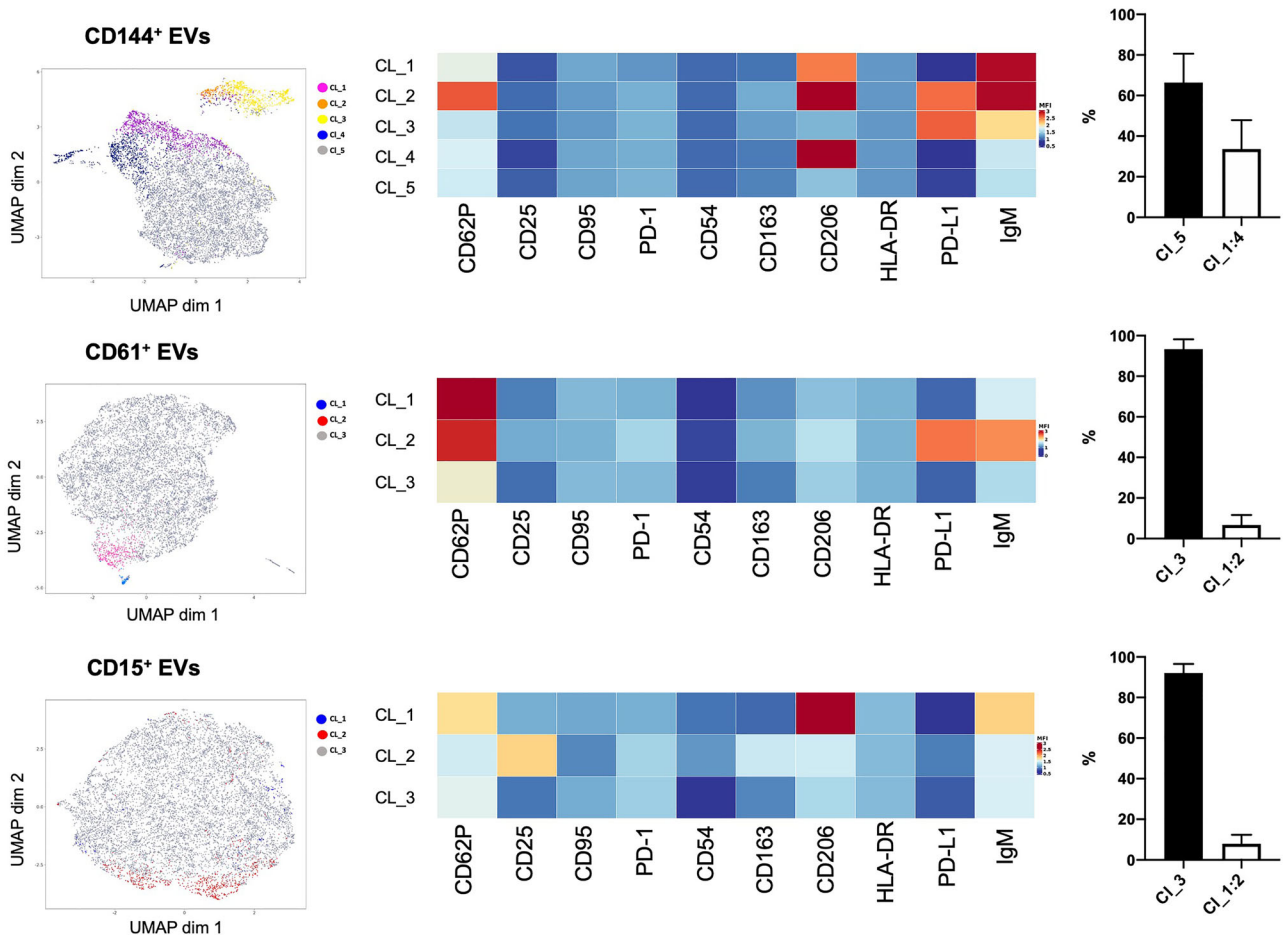


**FIGURE 4** | Unsupervised analysis of CD144<sup>+</sup>, CD61<sup>+</sup> and CD15<sup>+</sup> plasma EVs. The UMAP plot shows EV clusters of 16 merged samples; EVs were coloured according to the identified clusters. Heatmaps of Median Fluorescence Intensity (MFI) of the markers were used to identify clusters. The percentage of the major cluster and the other clusters among CD144<sup>+</sup>, CD61<sup>+</sup> and CD15<sup>+</sup> plasma EVs respectively were reported.

on CD61<sup>+</sup> EVs (Figure S10). However, whilst we cannot exclude the possibility that their composition differs—since tetraspanins are not ubiquitous markers of EVs—our findings suggest no substantial differences among the three EV subsets investigated. Overall, these data demonstrate the feasibility of performing deep multiparametric spectral flow cytometry analysis of EVs using fluorochromes with diverse chemical properties. Furthermore, the unsupervised analysis suggests an active release of heterogeneous EVs carrying up to five antigens, although the majority of EVs display only a single antigen on their surface, likely due to limited surface area or steric hindrance of the antibodies.

### 3.3 | Effect of Antibody Steric Hindrance on EV Immunophenotyping

The finding that a few EVs carried multiple antigens prompted us to investigate whether plasma-EV immunophenotyping could be affected by antibody steric hindrance. To address this topic, we first conducted experiments using EVs obtained from in vitro stimulated neutrophils.

More in detail, we stained neutrophil-derived EVs using antibodies that recognise four antigens expressed at a high density by neutrophils: CD15, CD16, CD45 and CD66b either individually

or mixed (Figure 5A). We observed minimal differences in the abundance of the four EV subsets when EVs were stained with antibodies individually versus in combination suggesting that steric hindrance plays a marginal role. Moreover, we assessed antigen co-expression on individual EVs by analysing the surface expression of CD45, CD66b, CD15 and CD16 on Neutrophil-derived EVs using imaging integrated flow cytometry (Figure S11). Our analysis revealed a high degree of heterogeneity, with EVs displaying one, two, three or all four markers. These findings suggest that EVs do not entirely reflect the phenotype of the cell from which they originate and support the notion of a low impact of antibody steric hindrance on EV phenotype.

To further substantiate this finding, we stained PBMC-derived EVs using antibodies recognising three antigens expressed at high density by T cells: CD3, CD4 and CD8 either individually or mixed. As shown before, we did not observe relevant fluctuations when comparing the abundance of CD3-derived, CD4-derived and CD8-derived EVs between the two staining conditions (Figure S12). Next, we proceeded to ex vivo experiments where we analysed plasma-CD144<sup>+</sup> EVs stained with anti-CD54, anti-PD-L1, CD206 or anti-CD62P individually paired with anti-CD144, or mixed altogether. We selected anti-CD54, anti-PD-L1, anti-CD206 and anti-CD62P from our antibody panel since they target antigens potentially expressed by endothelial cells under



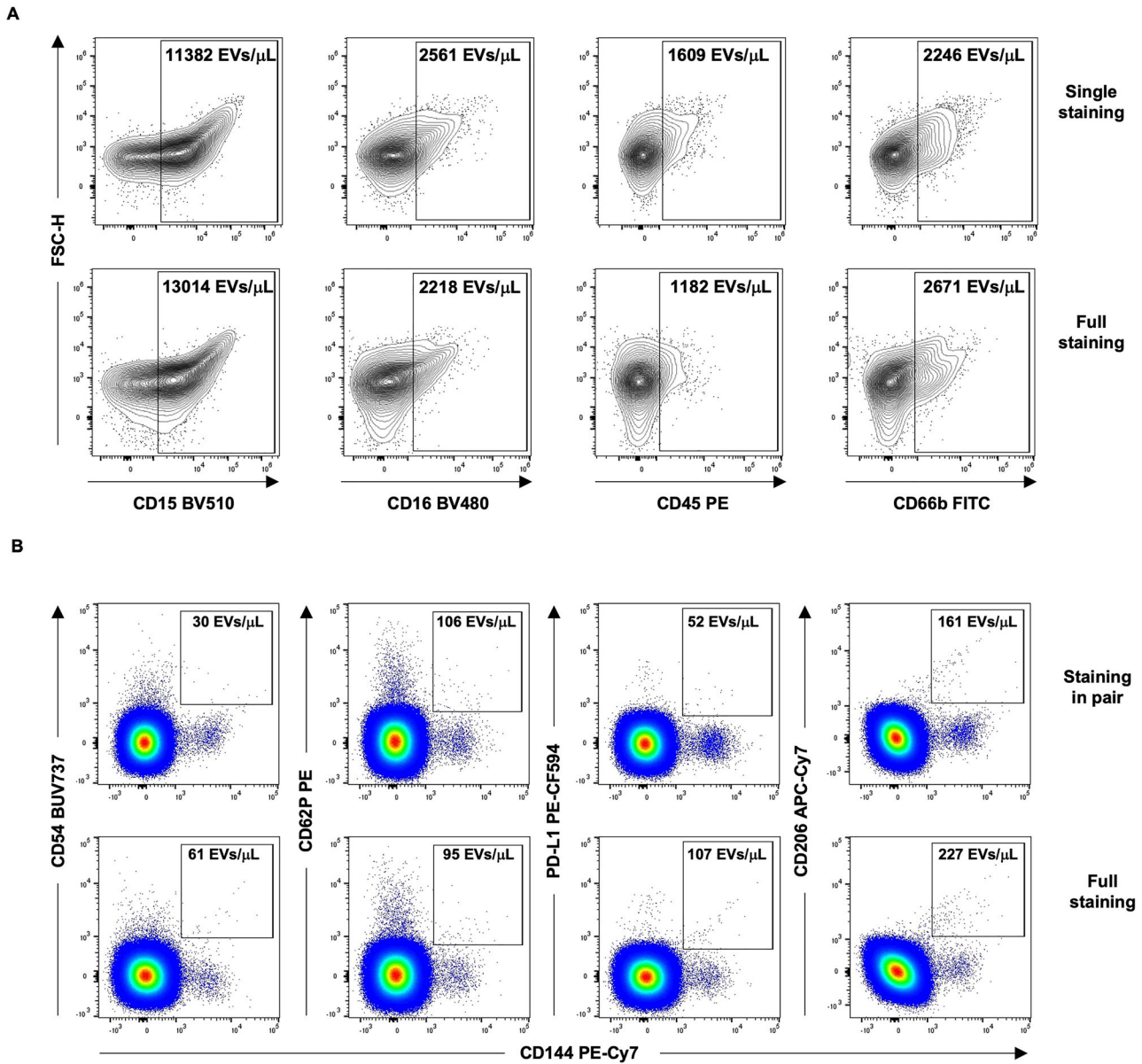


**FIGURE 5** | Effect of antibody steric hindrance on both in vitro and ex vivo EV immunophenotyping. EVs from in vitro stimulated neutrophils were stained using Phalloidin Alexa 647 plus the following antibodies: CD15 BV510, CD16 BV480, CD45 PE and CD66b FITC, either individually or in combination. Among the Phalloidin- events, the absolute counts of CD15<sup>+</sup>, CD16<sup>+</sup>, CD45<sup>+</sup> and CD66b<sup>+</sup> EVs/μL were reported (A). Data were representative of two independent observations. Plasma EVs were stained using Phalloidin Alexa 647 and the following antibodies: CD54 BUV737, CD206 APC-Cy7, PD-L1 PE-CF594 and CD62P PE, either paired with CD144 PE-Cy7 or in combination with CD144 PE-Cy7. Among the Phalloidin-negative events, the absolute counts of CD144<sup>+</sup>/CD54<sup>+</sup>, CD144<sup>+</sup>/CD206<sup>+</sup>, CD144<sup>+</sup>/PD-L1<sup>+</sup> and CD144<sup>+</sup>/CD62P<sup>+</sup> EVs/μL were reported (B). Data were representative of two independent observations.

pathophysiologic conditions. Additionally, in Figure 4 we had already identified subsets of CD144<sup>+</sup> EVs expressing most of these antigens.

As shown in Figure 5B, we did not observe any relevant fluctuation in the amount of PD-L1<sup>+</sup>/CD144<sup>+</sup> EVs, CD54<sup>+</sup>/CD144<sup>+</sup> EVs, CD206<sup>+</sup>/CD144<sup>+</sup> and CD62P<sup>+</sup>/CD144<sup>+</sup> EVs between the two staining conditions, confirming the results obtained from the in vitro experiments. Noteworthy, for these experiments we used fluorochromes with considerable heterogeneity in both molecular weight and chemical structure suggesting minimal fluorochrome-mediated side effects (Table S5). Altogether, these

data suggest that the phenotypic identification of the EV antigenic pattern is marginally influenced by the steric hindrance from either antibodies or fluorochromes. Noteworthy, both in vitro and ex vivo experiments support the idea that EVs carry a specific antigen repertoire upon release, as they do not precisely mirror the phenotype of their parent cells.

### 3.4 | Panel Testing on a Pilot Cohort of SLE Patients

After confirming the feasibility of a 21-colour panel for the analysis of plasma-derived EVs, we investigated the EV repertoire

in the plasma of a pilot cohort of SLE patients compared to HDs (Table S6).

To investigate EV phenotypes, we used a combination of manual gating and unsupervised analysis as described above. The data revealed the well-characterised EVs carrying lineage antigens, as well as EVs expressing molecules related to cell activation or exhaustion (Figure 6).

More specifically, we predominantly observed CD144<sup>+</sup>, CD61<sup>+</sup> and CD15<sup>+</sup> EVs among the lineage antigens, although their levels did not differ between patients and healthy subjects (Figure 6). Among the activation/exhaustion antigens, there was a significant increase of CD54<sup>+</sup> derived EVs in SLE patients as compared to HDs (Figure 6). CD54<sup>+</sup> EVs partially co-expressed only HLA-DR (SLE:  $9.6 \pm 5.3\%$ ; HD:  $15.1 \pm 8.2\%$ ;  $p = 0.16$ ) on their surface, further indicating a limited antigen repertoire carried by EVs. Moreover, the unsupervised analysis of CD144<sup>+</sup>, CD61<sup>+</sup> and CD15<sup>+</sup> EVs even showing new and poorly known EV subsets, did not reveal any significant difference between SLE and healthy subjects (Figure S13). Altogether these preliminary data support the notion of a heterogeneous active release of EVs in SLE.

## 4 | Discussion

Here, we significantly advance the field of EV analysis by describing the design, optimisation and initial application of a comprehensive high-parameter spectral flow cytometry protocol for the evaluation of circulating plasma EVs.

Spectral flow cytometry offers advantages such as an increased number of parameters and improved detection sensitivity as compared to conventional flow cytometry (Robinson 2019, Nolan 2022, Novo 2022). However, the EV flow cytometry analysis, even using a spectral approach, remain a challenge basically due to the EV small size and low refractive index. Indeed, EVs have signal intensities just below and above most of the instrument detection limit thus overlapping with buffer contaminants and unstained reagents (Welsh et al. 2021, Cook et al. 2023). Thus, we performed an instrument set up phase in which we optimised light scatter, fluorescence detector setting, ASF and WE using organo-silica beads or pre-stained EVs instead of polystyrene beads or cells thus maximising signal resolution. Our isolation approach might enrich samples with mainly large EVs. Therefore, despite this being, to our knowledge, the first manuscript aiming to perform instrument setup predominantly using EVs from stimulated primary cells, we cannot exclude the need for adjustments when integrated devices or new instruments capable of detecting particles smaller than 140–150 nm are used. In these cases, it would be necessary to adapt our flexible workflow to isolate smaller EV subpopulations, using methods such as ultracentrifugation or size-exclusion chromatography. Once we defined the best instrument set-up for EV flow cytometry analysis, we focused our efforts on panel design. Hitherto, EV immunophenotyping has been mainly performed using a short list of directly conjugated antibodies that recognise lineage markers (Anselmo et al. 2021, Anselmo et al. 2016, Suades et al. 2023, Falasca et al. 2021). Among fluorochrome options, researchers have often used either small organic dyes (i.e., FITC or Alexa dyes) or large protein-based molecules (PE or APC) because of their sufficient

brightness to ensure phenotyping of low number of surface proteins as well as good EV labelling efficiency and minimal fluorescence signal in solution (Welsh et al. 2023). However, during the last decade, the implementation of both conventional and spectral instruments equipped with an increasing number of laser sources, has contributed to the development of new class of fluorophores such as organic polymers (Chattopadhyay et al. 2012, Telford et al. 2019) potentially suitable for EV immunophenotyping. Hence, in the effort to build a 21-colour panel for an EV landscape analysis, we tested these new dyes following a specific fluorochrome performance metric. More in detail, we first investigated their brightness and in turn, their capability to detect EV-like events in the supernatant of in vitro stimulated PBMCs. Then, we assigned dim fluorochromes to lineage markers and the brightest ones to activation/exhaustion markers.

In terms of biology, the overreaching goal of this panel was to analyse deeply the plasma-derived EV repertoire in an effort to identify novel circulating biomarkers with a diagnostic or prognostic value. To this end, we set up a combination of the conventional 2D manual gating strategy and an unbiased approach thus potentially identifying EVs that co-expressed more than two antigens on their surface, as well as new, poorly described EV subsets. Unfortunately, we were not able to run a full unbiased analysis since the EV light scatter features did not allow a well discrimination of EVs from buffer contaminants, and the electronic noise. Thus, the general pipeline including sample cleaning, down sample, clustering and dimensionality (Moschetti et al. 2022, De Monte et al. 2023) reduction allowed only the detection of the most abundant EVs.

The unsupervised analysis performed on the main EV subsets (CD144<sup>+</sup>, CD61<sup>+</sup> and CD15<sup>+</sup> EVs) showed the expression of EVs carrying only lineage markers together with those also expressing activation/exhaustion markers. Interestingly, among endothelial-, platelet- and neutrophil-derived EVs, we observed clusters expressing the immunoglobulin IgM, the mannose receptor (CD206), P-selectin (CD62P) and/or the programmed cell death ligand-1 (PD-L1). However, since the soluble form of these molecules has been already described in body fluids (Justel et al. 2013, Bailly et al. 2021, Clemente et al. 2022, Blann 2014, Antonopoulos et al. 2014), they might be corona proteins formed spontaneously around the EV surface instead of originating from the parent cell (Tóth et al. 2021, Heidarzadeh et al. 2023). Moreover, we cannot formally exclude contamination of protein aggregates even though we avoided plasma centrifugation thus minimising the formation of biological artefacts (Tóth et al. 2021).

Furthermore, the low frequency of clusters showing more than one antigen on the EV surface prompted us to investigate the role of the antibody steric hindrance on the EV phenotype. Nowadays this topic is still under debate among those working on either EVs or cells (Welsh et al. 2023, De Vita et al. 2015). However, our data suggested a minimal effect of antibody steric hindrance on the EV phenotype, supporting the biological relevance of the observed antigen patterns, at least in our experimental conditions. Even though these results align with previous findings demonstrating the feasibility of a simultaneous expression of multiple antigens on the surface of plasma EVs (Karimi et al. 2022), the use of spatial-resolution techniques such as fluorescence resonance

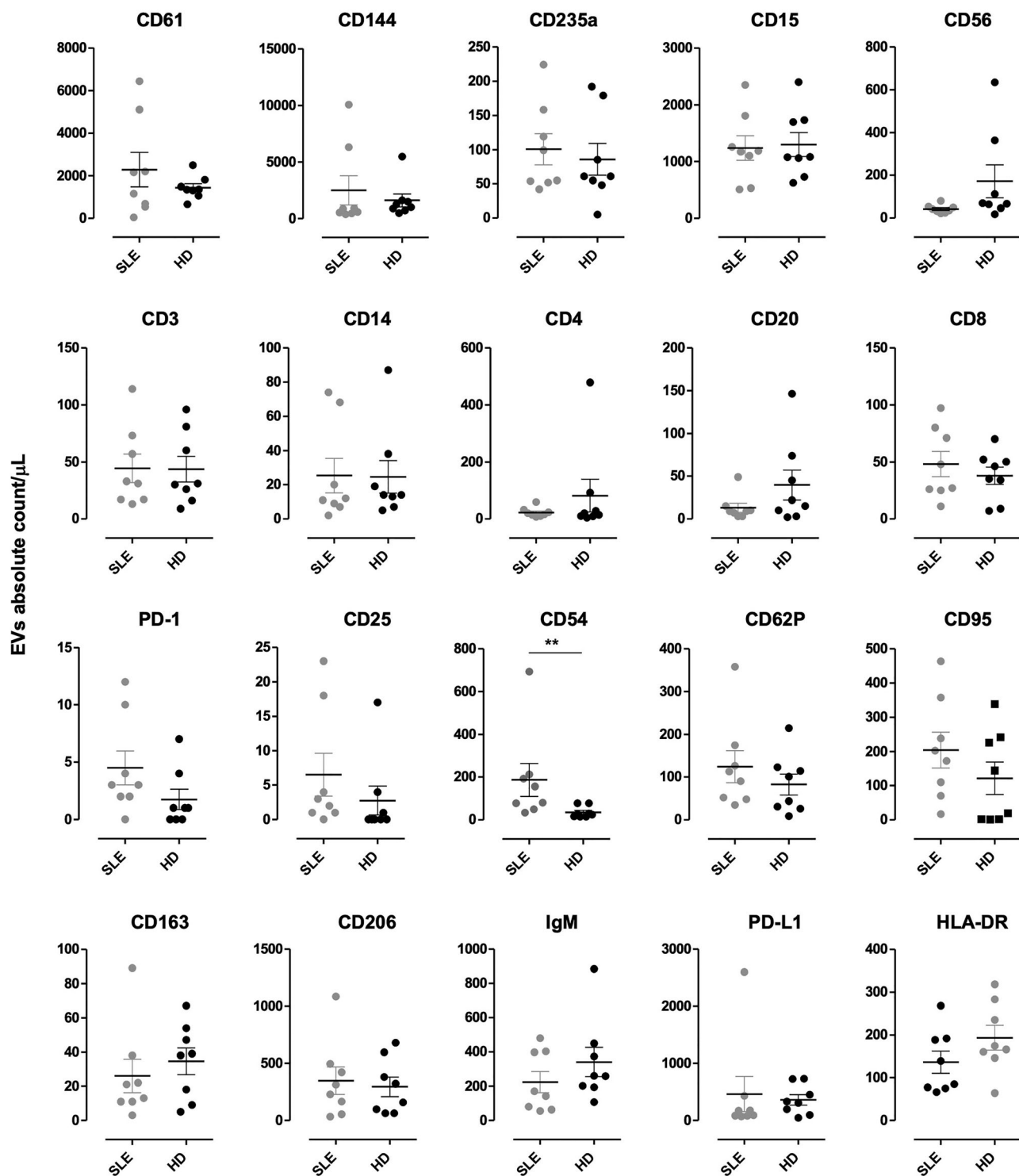


**FIGURE 6** | Quantification of circulating plasma EVs from Systemic Lupus Erythematosus patients and healthy donors. Platelets (CD61<sup>+</sup>), Endothelial (CD144<sup>+</sup>), Erythrocytes (CD235<sup>+</sup>), Neutrophils (CD15<sup>+</sup>), NK (CD56<sup>+</sup>), Lymphocytes (CD3<sup>+</sup>), Monocytes (CD14<sup>+</sup>), T-helper (CD4<sup>+</sup>), B cells (CD20<sup>+</sup>), Cytotoxic T cells (CD8<sup>+</sup>) derived-EVs and EVs expressing PD-1, CD25, CD54, CD62P, CD95, CD163, CD206, IgM, PD-L1 and HLA-DR were quantified using Cytex Aurora. EVs/ $\mu$ L were reported in the gated regions. Unpaired T Test (\*\* $p < 0.01$ ). Error bars represent the SD.

energy transfer (FRET) or super-resolution microscopy could further address the molecular co-localisation on distinct EVs within the same sample.

Recent evidence indicates EVs as active players in the pathogenesis and clinical complications of SLE (Nielsen et al. 2016).

Moreover, the immunophenotyping and quantification of EVs through flow cytometry have been of increasing interest to explore new circulating biomarkers useful for SLE disease diagnosis and prognosis (Mobarrez et al. 2019, Perez-Hernandez and Cortes 2015, Viñuela-Berni et al. 2015, López et al. 2017, Burbano et al. 2019, Lu et al. 2019).

As a preliminary result, we applied the 21-colour panel on plasma samples collected from a pilot cohort of SLE patients showing a significant increase of CD54<sup>+</sup> EVs as compared to HDs. Interestingly, these data are in line with recent evidence suggesting the role of soluble ICAM as an SLE biomarker (Yu et al. 2021, Egerer et al. 2000).

Notably, our spectral flow cytometry workflow, whilst validated in the context of SLE, has potential applications beyond this disease. The ability to perform high-dimensional immunophenotyping of EVs could provide valuable insights into various conditions where EVs serve as critical biomarkers such as cancer, cardiovascular diseases, neurological disorders and other autoimmune diseases (Anselmo et al. 2021, Withrow et al. 2016, Minciacchi et al. 2015, Shah et al. 2018)

As a limit of this pilot study, we cannot formally exclude that the low abundance of some EV subsets such as CD20<sup>+</sup> EVs or CD14<sup>+</sup> EVs was a consequence of the low plasma volume used for the staining or, more probably, simply related to the few numbers of samples analysed. The use of a panel with multiple antibody clones and 21 distinct fluorochromes makes it challenging to report the data in standardised units, preventing us from determining whether this setup would be optimal on other instruments. However, the tools employed for this setup can be applied by other laboratories using spectral analysers.

Altogether, these data highlight the value of a flow cytometry deep characterisation of circulating plasma EVs as a non-invasive “liquid biopsy” to potentially improve the knowledge of SLE pathophysiology as well as to perform a better assessment of patient risk stratification that could also develop into highly effective platforms for personalised medicine.

#### Author Contributions

**Daniela Boselli:** data curation, formal analysis, investigation, investigation, methodology, methodology, writing–review and editing, writing–review and editing. **Francesca Clemente:** data curation, formal analysis, methodology, writing–review and editing. **Simona Di Terlizzi:** formal analysis, methodology, writing–review and editing. **Christina Pagiatakis:** methodology. **Laura Papa:** methodology. **Genny Del Zotto:** methodology. **Chiara Villa:** funding acquisition, writing–review and editing. **Giuseppe Alvise Ramirez:** data curation, formal analysis, writing–review and editing. **Norma Maugeri:** data curation, funding acquisition, methodology, writing–review and editing. **Angelo A. Manfredi:** conceptualization, funding acquisition, project administration, supervision, writing–review and editing. **Achille Anselmo:** conceptualization, data curation, formal analysis, funding acquisition, investigation, methodology, project administration, supervision, visualization, writing–original draft, writing–review and editing

#### Acknowledgements

We would like to extend our gratitude to the volunteers who participated in this study. We acknowledge Enrico Ragni from IRCCS Istituto ortopedico Galeazzi, Milan, Italy for technical support.

Open access funding provided by BIBLIOSAN.

#### Conflicts of Interest

The authors declare no conflicts of interest.

#### Data Availability Statement

Data are available on request from the authors.

#### Declaration of Generative AI and AI-Assisted Technologies

During the preparation of this work, the author A.A. used ChatGPT 4.0 to revise the grammar and the style of some sentences.

#### References

- Anees, F., D. A. Montoya, D. S. Pisetsky, and C. K. Payne. 2024. “DNA Corona on Nanoparticles Leads to an Enhanced Immunostimulatory Effect With Implications for Autoimmune Diseases.” *PNAS* 121, no. 11: e2319634121.
- Anselmo, A., D. Frank, L. Papa, et al. 2021. “Myocardial Hypoxic Stress Mediates Functional Cardiac Extracellular Vesicle Release.” *European Heart Journal* 42, no. 28: 2780–2792.
- Anselmo, A., F. Riva, S. Gentile, et al. 2016. “Expression and Function of IL-1R8 (TIR8/SIGIRR), a Regulatory Member of the IL-1 Receptor Family in Platelets.” *European Journal of Immunology* 46: 416.
- Antonopoulos, C. N., G. S. Sfyroeras, J. D. Kakisis, K. G. Moulakakis, and C. D. Liapis. 2014. “The Role of Soluble P Selectin in the Diagnosis of Venous Thromboembolism.” *Thrombosis Research* 133, no. 1: 17–24.
- Arraud, N., C. Gounou, D. Turpin, and A. R. Brisson. 2016. “Fluorescence Triggering: A General Strategy for Enumerating and Phenotyping Extracellular Vesicles by Flow Cytometry.” *Cytometry Part A: The Journal of the International Society for Analytical Cytology* 89, no. 2: 184–195.
- Bailly, C., X. Thuru, and B. Quesnel. 2021. “Soluble Programmed Death Ligand-1 (sPD-L1): A Pool of Circulating Proteins Implicated in Health and Diseases.” *Cancers (Basel)* 13, no. 12: 3034–3058.
- Blann, A. D. 2014. “Soluble P-Selectin: The next Step.” *Thrombosis Research* 133, no. 1: 3–4.
- Brittain, G. C., Y. Q. Chen, E. Martinez, et al. 2019. “A Novel Semiconductor-Based Flow Cytometer With Enhanced Light-Scatter Sensitivity for the Analysis of Biological Nanoparticles.” *Scientific Reports* 9, no. 1: 16039.
- Burbano, C., J. A. Gómez-Puerta, C. Muñoz-Vahos, et al. 2019. “HMGB1(+) Microparticles Present in Urine Are Hallmarks of Nephritis in Patients With Systemic Lupus Erythematosus.” *European Journal of Immunology* 49, no. 2: 323–335.
- Chattopadhyay, P. K., B. Gaylord, A. Palmer, et al. 2012. “Brilliant Violet Fluorophores: A New Class of Ultrabright Fluorescent Compounds for Immunofluorescence Experiments.” *Cytometry Part A: The Journal of the International Society for Analytical Cytology* 81A, no. 6: 456–466.
- Clemente, E., M. Martinez-Moro, D. N. Trinh, et al. 2022. “Probing the Glycans Accessibility in the Nanoparticle Biomolecular Corona.” *Journal of Colloid & Interface Science* 613: 563–574.
- Cook, S., V. A. Tang, J. Lannigan, J. C. Jones, and J. A. Welsh. 2023. “Quantitative Flow Cytometry Enables End-to-End Optimization of Cross-Platform Extracellular Vesicle Studies.” *Cell Reports Methods* 3, no. 12: 100664.
- Cossarizza, A., H.-D. Chang, A. Radbruch, et al. 2019. “Guidelines for the Use of Flow Cytometry and Cell Sorting in Immunological Studies (Second Edition).” *European Journal of Immunology* 49, no. 10: 1457–1973.
- Crawford, J. D., H. Wang, D. Trejo-Zambrano, et al. 2023. “The XIST lncRNA Is a Sex-Specific Reservoir of TLR7 Ligands in SLE.” *JCI Insight* 8, no. 20: 169344–169362.
- Dasgupta, S. K., H. Abdel-Monem, P. Niravath, et al. 2009. “Lactadherin and Clearance of Platelet-Derived Microvesicles.” *Blood* 113, no. 6: 1332–1339.
- De Monte, L., F. Clemente, E. Ruggiero, et al. 2023. “Pro-Tumor Tfh2 Cells Induce Detrimental IgG4 Production and PGE(2)-Dependent IgE Inhibition in Pancreatic Cancer.” *EBioMedicine* 97: 104819.



- De Vita, M., V. Catzola, A. Buzzonetti, et al. 2015. "Unexpected Interference in Cell Surface Staining by Monoclonal Antibodies to Unrelated Antigens." *Cytometry Part B, Clinical Cytometry* 88, no. 5: 352–354.
- Diehl, P., A. Fricke, L. Sander, et al. 2012. "Microparticles: Major Transport Vehicles for Distinct microRNAs in Circulation." *Cardiovascular Research* 93, no. 4: 633–644.
- Egerer, K., E. Feist, U. Rohr, A. Pruss, G.-R. Burmester, and T. Dörner. 2000. "Increased Serum Soluble CD14, ICAM-1 and E-Selectin Correlate With Disease Activity and Prognosis in Systemic Lupus Erythematosus." *Lupus* 9, no. 8: 614–621.
- Falasca, K., P. Lanuti, C. Ucciferri, et al. 2021. "Circulating Extracellular Vesicles as New Inflammation Marker in HIV Infection." *AIDS* 35, no. 4: 595–604.
- Gladman, D. D., D. Ibanez, and M. B. Urowitz. 2002. "Systemic Lupus erythematosus Disease Activity index 2000." *Journal of Rheumatology* 29, no. 2: 288–291.
- Gul, B., F. Syed, S. Khan, A. Iqbal, and I. Ahmad. 2022. "Characterization of Extracellular Vesicles by Flow Cytometry: Challenges and Promises." *Micron (Oxford, England: 1993)* 161: 103341.
- Haraszti, R. A., M.-C. Didiot, E. Sapp, et al. 2016. "High-Resolution Proteomic and Lipidomic Analysis of Exosomes and Microvesicles From Different Cell Sources." *Journal of Extracellular Vesicles* 5: 32570.
- Heidarzadeh, M., A. Zarebkohan, R. Rahbarghazi, and E. Sokullu. 2023. "Protein Corona and Exosomes: New Challenges and Prospects." *Cell Communication and Signaling* 21, no. 1: 64.
- Hunter, M. P., N. Ismail, X. Zhang, et al. 2008. "Detection of microRNA Expression in human Peripheral Blood Microvesicles." *PLoS ONE* 3, no. 11: e3694.
- Justel, M., L. Socias, R. Almansa, et al. 2013. "IgM Levels in Plasma Predict Outcome in Severe Pandemic Influenza." *Journal of Clinical Virology* 58, no. 3: 564–567.
- Karimi, N., R. Dalirfardouei, T. Dias, J. Lötvall, and C. Lässer. 2022. "Tetraspanins Distinguish Separate Extracellular Vesicle Subpopulations in human Serum and Plasma—Contributions of Platelet Extracellular Vesicles in Plasma Samples." *Journal of Extracellular Vesicles* 11, no. 5: e12213.
- Karlsson, J., J. Wetterö, L. A. Potempa, et al. 2023. "Extracellular Vesicles Opsonized by Monomeric C-Reactive Protein (CRP) Are Accessible as Autoantigens in Patients With Systemic Lupus Erythematosus and Associate With Autoantibodies Against CRP." *Journal of Autoimmunity* 139: 103073.
- Kok, V. C., and C. C. Yu. 2020. "Cancer-Derived Exosomes: Their Role in Cancer Biology and Biomarker Development." *International Journal of Nanomedicine* 15: 8019–8036.
- López, P., J. Rodríguez-Carrio, A. Martínez-Zapico, L. Caminal-Montero, and A. Suárez. 2017. "Circulating Microparticle Subpopulations in Systemic Lupus Erythematosus Are Affected by Disease Activity." *International Journal of Cardiology* 236: 138–144.
- Loyer, X., A.-C. Vion, A. Tedgui, and C. M. Boulanger. 2014. "Microvesicles as Cell-Cell Messengers in Cardiovascular Diseases." *Circulation Research* 114, no. 2: 345–353.
- Lu, J., Z. B. Hu, P. P. Chen, et al. 2019. "Urinary Podocyte Microparticles Are Associated With Disease Activity and Renal Injury in Systemic Lupus Erythematosus." *BMC Nephrology [Electronic Resource]* 20, no. 1: 303.
- Manfredi, A. A., G. A. Ramirez, C. Godino, et al. 2022. "Platelet Phagocytosis via P-Selectin Glycoprotein Ligand 1 and Accumulation of Microparticles in Systemic Sclerosis." *Arthritis & Rheumatology* 74, no. 2: 318–328.
- Maugeri, N., M. Brambilla, M. Camera, et al. 2006. "Human Polymorphonuclear Leukocytes Produce and Express Functional Tissue Factor Upon Stimulation." *Journal of Thrombosis and Haemostasis* 4, no. 6: 1323–1330.
- Maugeri, N., L. Campana, M. Gavina, et al. 2014. "Activated Platelets Present High Mobility Group Box 1 to Neutrophils, Inducing Autophagy and Promoting the Extrusion of Neutrophil Extracellular Traps." *Journal of Thrombosis and Haemostasis* 12, no. 12: 2074–2088.
- McVey, M. J., C. M. Spring, and W. M. Kuebler. 2018. "Improved Resolution in Extracellular Vesicle Populations Using 405 Instead of 488 Nm Side Scatter." *Journal of Extracellular Vesicles* 7, no. 1: 1454776.
- Minciacchi, V. R., M. R. Freeman, and D. Di Vizio. 2015. "Extracellular Vesicles in Cancer: Exosomes, Microvesicles and the Emerging Role of Large Oncosomes." *Seminars in Cell & Developmental Biology* 40: 41–51.
- Mobarrez, F., E. Fuzzi, I. Gunnarsson, et al. 2019. "Microparticles in the Blood of Patients With SLE: Size, Content of Mitochondria and Role in Circulating Immune Complexes." *Journal of Autoimmunity* 102: 142–149.
- Moschetti, G., C. Vasco, F. Clemente, et al. 2022. "Deep Phenotyping of T-Cells Derived from the Aneurysm Wall in a Pediatric Case of Subarachnoid Hemorrhage." *Frontiers in Immunology* 13: 866558.
- Nielsen, C. T., N. S. Rasmussen, N. H. H. Heegaard, and S. Jacobsen. 2016. "'Kill' the Messenger: Targeting of Cell-Derived Microparticles in Lupus Nephritis." *Autoimmunity Reviews* 15, no. 7: 719–725.
- Nolan, J. P. 2022. "The Evolution of Spectral Flow Cytometry." *Cytometry Part A: The Journal of the International Society for Analytical Cytology* 101, no. 10: 812–817.
- Novo, D. 2022. "A Comparison of Spectral Unmixing to Conventional Compensation for the Calculation of Fluorochrome Abundances From Flow Cytometric Data." *Cytometry Part A: The Journal of the International Society for Analytical Cytology* 101, no. 11: 885–891.
- Nowicka, M., C. Krieg, L. M. Weber, et al. 2017. "CyTOF Workflow: Differential Discovery in High-Throughput High-Dimensional Cytometry Datasets." *F1000Research* 6: 748.
- Panagopoulou, M. S., A. W. Wark, D. J. S. Birch, and C. D. Gregory. 2020. "Phenotypic Analysis of Extracellular Vesicles: A Review on the Applications of Fluorescence." *Journal of Extracellular Vesicles* 9, no. 1: 1710020.
- Perez-Hernandez, J., and R. Cortes. 2015. "Extracellular Vesicles as Biomarkers of Systemic Lupus Erythematosus." *Disease Markers* 2015: 613536.
- Petri, M., A.-M. Orbai, G. S. Alarcón, et al. 2012. "Derivation and Validation of the Systemic Lupus International Collaborating Clinics Classification Criteria for Systemic Lupus Erythematosus." *Arthritis and Rheumatism* 64, no. 8: 2677–2686.
- Pisetsky, D. S. 2024. "Unique Interplay Between Antinuclear Antibodies and Nuclear Molecules in the Pathogenesis of Systemic Lupus Erythematosus." *Arthritis & Rheumatology* 76: 1334–1343.
- Rahman, A., and D. A. Isenberg. 2008. "Systemic Lupus Erythematosus." *New England Journal of Medicine* 358, no. 9: 929–939.
- Robbins, P. D., A. Dorronsoro, and C. N. Booker. 2016. "Regulation of Chronic Inflammatory and Immune Processes by Extracellular Vesicles." *Journal of Clinical Investigation* 126, no. 4: 1173–1180.
- Robinson, J. P. 2019. "Spectral Flow Cytometry—Quo Vadimus?" *Cytometry Part A: The Journal of the International Society for Analytical Cytology* 95, no. 8: 823–824.
- Shah, R., T. Patel, and J. E. Freedman. 2018. "Circulating Extracellular Vesicles in Human Disease." *New England Journal of Medicine* 379, no. 10: 958–966.
- Stoll, T., B. Seifert, and D. A. Isenberg. 1996. "SLICC/ACR Damage Index Is Valid, and Renal and Pulmonary Organ Scores Are Predictors of Severe Outcome in Patients With Systemic Lupus Erythematosus." *British Journal of Rheumatology* 35, no. 3: 248–254.
- Suades, R., A. Vilella-Figuerola, T. Padró, et al. 2023. "Red Blood Cells and Endothelium Derived Circulating Extracellular Vesicles in Health and Chronic Heart Failure: A Focus on Phosphatidylserine Dynamics

in Vesiculation.” *International Journal of Molecular Sciences* 24, no. 14: 11824–11839.

Telford, W., T. Georges, C. Miller, and P. Voluer. 2019. “Deep Ultraviolet Lasers for Flow Cytometry.” *Cytometry Part A: The Journal of the International Society for Analytical Cytology* 95, no. 2: 227–233.

Théry, C., K. W. Witwer, E. Aikawa, et al. 2018. “Minimal Information for Studies of Extracellular Vesicles 2018 (MISEV2018): A Position Statement of the International Society for Extracellular Vesicles and Update of the MISEV2014 Guidelines.” *Journal of Extracellular Vesicles* 7, no. 1: 1535750.

Tóth, E. Á., L. Turiák, T. Visnovitz, et al. 2021. “Formation of a Protein Corona on the Surface of Extracellular Vesicles in Blood Plasma.” *Journal of Extracellular Vesicles* 10, no. 11: e12140.

Tsokos, G. C. 2011. “Systemic Lupus Erythematosus.” *New England Journal of Medicine* 365, no. 22: 2110–2121.

van der Pol, E., T. G. van Leeuwen, and X. Yan. 2021. “Misinterpretation of Solid Sphere Equivalent Refractive Index Measurements and Smallest Detectable Diameters of Extracellular Vesicles by Flow Cytometry.” *Scientific Reports* 11, no. 1: 24151.

van Vollenhoven, R. F., G. Bertsias, A. Doria, et al. 2021. “2021 DORIS Definition of Remission in SLE: Final Recommendations From an International Task Force.” *Lupus Science & Medicine* 8, no. 1: 538–546.

Verderio, C., M. Gabrielli, and P. Giussani. 2018. “Role of Sphingolipids in the Biogenesis and Biological Activity of Extracellular Vesicles.” *Journal of Lipid Research* 59, no. 8: 1325–1340.

Viñuela-Berni, V., L. Doníz-Padilla, N. Figueroa-Vega, et al. 2015. “Proportions of Several Types of Plasma and Urine Microparticles Are Increased in Patients With Rheumatoid Arthritis With Active Disease.” *Clinical and Experimental Immunology* 180, no. 3: 442–451.

Vion, A.-C., B. Ramkhelawon, X. Loyer, et al. 2013. “Shear Stress Regulates Endothelial Microparticle Release.” *Circulation Research* 112, no. 10: 1323–1333.

Welsh, J. A., G. J. A. Arkesteijn, M. Bremer, et al. 2023. “A Compendium of Single Extracellular Vesicle Flow Cytometry.” *Journal of Extracellular Vesicles* 12, no. 2: e12299.

Welsh, J. A., D. C. I. Goberdhan, L. O’driscoll, et al. 2024. “Minimal Information for Studies of Extracellular Vesicles (MISEV2023): From Basic to Advanced Approaches.” *Journal of Extracellular Vesicles* 13, no. 2: e12404.

Welsh, J. A., V. A. Tang, E. Van Der Pol, and A. Görgens. 2021. “MIFlowCyt-EV: The Next Chapter in the Reporting and Reliability of Single Extracellular Vesicle Flow Cytometry Experiments.” *Cytometry Part A: The journal of the International Society for Analytical Cytology* 99, no. 4: 365–368.

Withrow, J., C. Murphy, Y. Liu, M. Hunter, S. Fulzele, and M. W. Hamrick. 2016. “Extracellular Vesicles in the Pathogenesis of Rheumatoid Arthritis and Osteoarthritis.” *Arthritis Research & Therapy* 18, no. 1: 286.

Xu, R., D. W. Greening, H.-J. Zhu, N. Takahashi, and R. J. Simpson. 2016. “Extracellular Vesicle Isolation and Characterization: Toward Clinical Application.” *Journal of Clinical Investigation* 126, no. 4: 1152–1162.

Yáñez-Mó, M., P. R.-M. Siljander, Z. Andreu, et al. 2015. “Biological Properties of Extracellular Vesicles and Their Physiological Functions.” *Journal of Extracellular Vesicles* 4: 27066.

Yu, K. Y., S. Yung, M. K. Chau, et al. 2021. “Clinico-Pathological Associations of Serum VCAM-1 and ICAM-1 Levels in Patients With Lupus Nephritis.” *Lupus* 30, no. 7: 1039–1050.

Zhao, Y., W. Wei, and M.-L. Liu. 2020. “Extracellular Vesicles and Lupus Nephritis.” *Journal of Autoimmunity* 115: 102540.

## Supporting Information

Additional supporting information can be found online in the Supporting Information section.